

Influence of replacement of Mn by Cr on magnetocaloric properties of quenched NiMn_{1-x}Cr_xGe alloys

E. Zubov^{1,2}, N. Nedelko³, A. Sivachenko⁴, K. Dyakonov⁵, Yu. Tyvanchuk⁶, M. Marzec⁶, V. Valkov⁴, W. Bażela⁸, A. Ślawska-Waniewska³, V. Dyakonov³, A. Szytuła⁷, and H. Szymczak³

¹*G.V. Kurdyumov Institute for Metal Physics, NASU, 36 Acad. Vernadsky Boulevard, Kyiv 03680, Ukraine*
E-mail: eezubov@ukr.net

²*Vasyl' Stus Donetsk National University, Vinnytsia 21021, Ukraine*

³*Institute of Physics, PAS, 32/46 Al. Lotników, Warsaw 02-668, Poland*

⁴*O.O. Galkin Donetsk Institute of Physics and Engineering, 46 Nauki Ave., Kyiv 03680, Ukraine*

⁵*Ioffe Physico-Technical Institute RAS, St.-Petersburg 194021, Russia*

⁶*Faculty of Chemistry, Ivan Franko National University of Lviv, 6 Kyryla i Mephodia Str., Lviv 79005, Ukraine*

⁷*Institute of Physics, Jagiellonian University, 4 Reymonta, Kraków 30-059, Poland*

⁸*Institute of Physics, Krakow University of Technology, 1 Podchorążych, Kraków 30-084, Poland*

Received April 13, 2018, published online June 27, 2018

In this paper, the crystallographic, magnetic, thermomagnetic, and magnetocaloric properties of the quenched NiMn_{1-x}Cr_xGe ($x = 0.04, 0.18$ and 0.25) half-Heusler alloys have been studied by x-ray diffraction, differential scanning calorimetry and magnetization measurements. An influence of partial substitution of Cr for Mn and quenching of the samples on the character of structural and magnetic phase transitions is presented. Quenching of the alloys results in the formation of two phase (orthorhombic and hexagonal) crystal structure. The magnetic properties were investigated by means of magnetization measurements over a wide temperature (5–400 K) and magnetic field (up to 60 kOe) ranges. The experimental data indicate that at quenching and with increasing Cr content the magnetic order changes from antiferromagnetic to ferromagnetic. Hardened compounds exhibit a thermal hysteresis in the vicinity of the magnetic phase transition, what is characteristic for a first-order magnetic phase transition. The magnetic phase transition temperatures are decreased as a result of quenching of the samples. The magnetic entropy changes were calculated using the field dependences of isothermal magnetization in terms of the thermodynamic Maxwell relation. The magnetic entropy changes, $|\Delta S_M^{\max}|$, obtained for the hardened alloys with $x = 0.25$ have the maximum value equal to 23 J/(kg·K) near the magnetic phase transition for a field change of $\Delta H = 0-60$ kOe.

PACS: 75.30.Sg Magnetocaloric effect, magnetic cooling;
75.30.Kz Magnetic phase boundaries (including classical and quantum magnetic transitions, metamagnetism, etc.);
75.30.Gw Magnetic anisotropy;
75.47.Np Metals and alloys;
75.50.Ee Antiferromagnetics;
75.60.Ej Magnetization curves, hysteresis, Barkhausen and related effects;
65.40.gd Entropy.

Keywords: intermetallic alloys NiMn_{1-x}Cr_xGe, magnetization, magnetic phase transition, magnetic entropy, magnetocaloric effect.

1. Introduction

Magnetic materials showing the large changes in the magnetic entropy of a system in an applied magnetic field are of particular interest, since magnetic refrigeration based on the magnetocaloric effect (MCE) is highly energy efficient and can serve as a perspective alternative for traditional refrigeration technology.

Theoretical, technological and experimental efforts were made to find the magnetic refrigerants working effectively near ambient temperatures. The magnetic entropy changes are established to be greatly enhanced in case of a first-order paramagnetic (PM) to ferromagnetic (FM) phase transition compared to a second-order one. A large MCE near the room temperature due to a first-order magnetic phase transition was discovered in a wide series of materials, including the lanthanum–manganese–perovskite oxides $\text{La}_{1-x}(\text{Ca,Sr})_x\text{MnO}_x$ [1], transition metal-based alloys such as $\text{Mn}_{2-x}\text{Fe}_x\text{P}_{1-y}\text{As}_y$ [2] as well as a new class of half-Heusler materials of $\text{MM}'\text{X}$ type, where M and M' are a 3d electron elements and X is Si or Ge. Among them, especially interesting are the intermetallic $\text{MnNi}_{1-x}\text{Co}_x\text{Ge}$ [3], $\text{Mn}_{1-x}\text{Cr}_x\text{CoGe}$ [4], $\text{Ni}_{1-x}\text{Co}_x\text{MnGe}_{1.05}$ [5], $\text{Mn}_{1-x}\text{Cr}_x\text{NiGe}_{1.05}$ [6] and $\text{Mn}_{0.89}\text{Cr}_{0.11}\text{NiGe}$ [7,8] alloys isostructural with the NiMnGe alloy. These alloys possess the large magnetocaloric effect due to strong coupling between magnetic and lattice systems as well as due to coupling of the magnetic sublattice with magnetic field, which changes the magnetic part of entropy of materials.

The x-ray and neutron powder diffraction data show that in the NiMnGe alloy the structural transition (at $T_m = 470$ K) from a high-temperature hexagonal phase of the NiIn₂-type (space group $P6_3/mmc$) to a low-temperature orthorhombic structure of the TiNiSi-type (space group $Pnma$) takes place [9,10]. In the NiMnGe alloy the magnetic phase transition from paramagnetic phase to antiferromagnetic (AFM) spiral structure at the Neel temperature of $T_N = 346$ K is observed [11,12]. Substitution of Mn by other 3d elements results in a change of the magnetic state of the system. For example, the magnetic ordering of the $\text{NiMn}_{1-x}\text{Ti}_x\text{Ge}$ alloys changes with increasing x from antiferromagnetic state for $x \leq 0.1$ to ferromagnetic one for $0.15 < x < 0.65$ and paramagnetic state for higher concentrations of Ti [13]. At substitution of Ni by another 3d element a ferromagnetic order in $\text{Co}_x\text{Ni}_{1-x}\text{MnGe}$ is stable above $x = 0.2$ [9]. The hexagonal $\text{Mn}_{1-x}\text{Cr}_x\text{CoGe}$ [4], $\text{Ni}_{1-x}\text{Co}_x\text{MnGe}_{1.05}$ [5], $\text{Mn}_{1-x}\text{Cr}_x\text{NiGe}_{1.05}$ [6] and $\text{Mn}_{0.89}\text{Cr}_{0.11}\text{NiGe}$ [7,8] compounds have a first order ferromagnetic phase transition with the Curie temperature (T_C) close to room temperature. The magnetic properties and the magnetic ordering temperature of these intermetallic alloys were found to be controlled by varying Mn/Cr ratio and thermal treatment.

The results for the slowly cooled samples $\text{NiMn}_{1-x}\text{Cr}_x\text{Ge}$ indicate orthorhombic crystal structure, change of magnetic

properties from antiferro- to ferromagnetic and increase of the maximum entropy with the increasing of Cr content [14].

In parallel with scientific interest, these compounds have attracted also practical interest due to their large magnetocaloric effect.

In the present work, the crystallographic, magnetic, thermomagnetic properties and MCE in the hardened $\text{NiMn}_{1-x}\text{Cr}_x\text{Ge}$ ($x = 0.04, 0.18$ and 0.25) compounds as a function of temperature and external magnetic field have been studied. These compounds constitute a class of systems that is important for fundamental research due to the diversity of their magnetic and structural properties. An interest in the studies of these compounds was motivated mainly by attempt to study an influence of both substitution of Mn for Cr and hardening on their magnetocaloric properties. It has to be mentioned that in contrast with other MCE materials, the studied compounds do not contain the toxic constituent (as in the MnFePAs systems [2]) or the expensive rare-earth element Gd (as in the $\text{Gd}_5\text{Si}_2\text{Ge}_2$ family [15]). In studied alloys the magnetic phase transition temperatures are near to room temperature. Such features have served as an incentive for a search of new intermetallic materials displaying the large MCE.

We have observed strong dependence of MCE on Cr content and quenching of the samples. The results obtained reinforce and extend the already existing data on the magnetism of intermetallic materials as well as show that these alloys can be a promising candidate for future room-temperature magnetic refrigeration.

2. Samples preparation and experimental details

The magnetic measurements have been performed on the polycrystalline samples with general formula of $\text{NiMn}_{1-x}\text{Cr}_x\text{Ge}$ ($x = 0.04, 0.18$ and 0.25). The studied alloys were prepared by induction twofold re-melting of mixture of high purity Mn, Cr, Ni, Ge elements taken in corresponding proportions. The resulting ingots were placed in the sealed quartz ampoules in argon atmosphere under the vacuum of 10^{-3} Torr. A homogenization process as a result of an annealing of ingot at temperature of 850 K for 48 hours was performed. Then the obtained alloys were quenched in water.

The crystallographic structures were examined by using the x-ray powder diffraction method on Empyrean 2 (PANalytical) diffractometer with CuK_α radiation at room temperature. The x-ray diffraction data were analyzed using FullProf program [14].

The differential scanning calorimetry (DSC) measurements were carried out using a Perkin Elmer Pyris 1 DSC calorimeter in the temperature range of 100–420 K with the temperature change of 10 K/min during heating and cooling with the temperature rate of 20 K/min.

The field and temperature dependences of dc magnetization were measured in a wide temperature (5–400 K) and magnetic field (up to 60 kOe) ranges using a Quantum

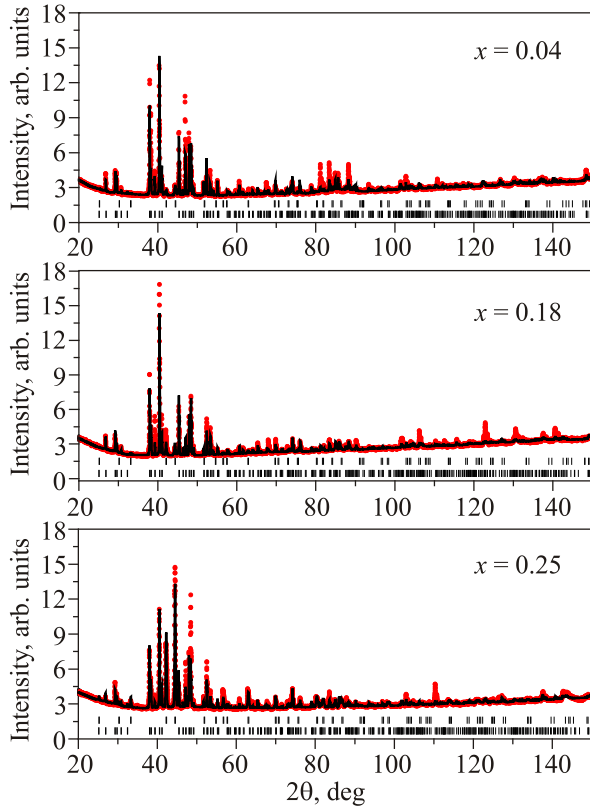


Fig. 1. (Color online) The x-ray diffraction patterns of the hardened samples for $x = 0.04, 0.18, 0.25$ collected at room temperature. Vertical bars correspond to Bragg reflections from hexagonal structure (upper row) and from orthorhombic structure (lower row). The difference between the experiment and the Rietveld refinement results is plotted in the bottom of each diffraction pattern.

Design PPMS platform equipped with a vibrating sample magnetometer. $M(T)$ curves were recorded at $H = 100$ Oe on cooling and heating processes. Isothermal magnetization curves were measured with temperature steps of 2–3 K over a temperature range around the magnetic phase transition.

3. Structural properties

The x-ray diffraction patterns of the hardened NiMn_{1-x}Cr_xGe samples with $x = 0.04, 0.18$ and 0.25 collected at room temperature are presented in Fig. 1.

The x-ray diffraction data at room temperature show that compounds have two-phase orthorhombic of TiNiSi-type and hexagonal of the Ni₂In-type states for $x = 0.18$ and 0.25 . The volume fraction of orthorhombic and hexagonal phases was calculated by Rietveld refinement using the FULLPROF package. At room temperature the relation between hexagonal (H) and orthorhombic (O) phases depends on Cr concentration, namely, for $x = 0.04$ — 95%(O)+5%(H), $x = 0.18$ — 91%(O)+9%(H) and $x = 0.25$ — 53%(O)+47%(H).

The lattice parameters and unit-cell volume, V , of the hexagonal and orthorhombic phases collected at room temperature are listed in Table 1. With increase of the Cr (x) content the unit-cell volumes in both phases decrease.

4. Magnetic properties

The temperature dependences of field-cooled (FC) and field-heated (FH) magnetization for the samples with various Cr content measured in magnetic field of 100 Oe demonstrate that for all the samples a separation between FC and FH $M(T)$ curves is observed (see Fig. 2).

The FC $M(T)$ curve for the sample with $x = 0.04$ has a maximum of magnetization at T_N temperature equal to 344 K corresponding to the PM–AFM transition. Observed for $x = 0.18$ and 0.25 compounds magnetization behavior indicate the ferromagnetic character of spin order. The $M(T)$ curves are seen to shift towards low temperatures as a result of increasing of Cr content. A large temperature hysteresis of the $M(T)$ curves is indicative of a first-order PM–FM phase transitions.

An increase in Cr concentration results in a significant decrease of the Curie temperature (Table 2). At high temperatures the reciprocal magnetic susceptibility, $H/M(T)$, obeys the Curie–Weiss law. As is shown in Table 2, the paramagnetic Curie temperature, Θ , has a positive sign that is indicative of dominant ferromagnetic interactions.

Table 1. Lattice parameters of the hexagonal and orthorhombic phases of the quenched NiMn_{1-x}Cr_xGe samples at room temperature

Content, x	Structure type of phase	Space group	a , Å	b , Å	c , Å	V , Å ³
0.04	Ni ₂ In	$P6_3/mmc$	4.0804(4)	–	5.4171(10)	78.11(3)
	TiNiSi	$Pnma$	6.0292(2)	3.75912(7)	7.0811(2)	160.489(10)
0.18	Ni ₂ In	$P6_3/mmc$	4.0821(3)	–	5.3965(6)	77.88(2)
	TiNiSi	$Pnma$	6.0129(2)	3.7559(1)	7.0770(2)	159.83(2)
0.25	Ni ₂ In	$P6_3/mmc$	4.0747(2)	–	5.3848(3)	77.43(1)
	TiNiSi	$Pnma$	6.0076(3)	3.7568(2)	7.0763(3)	159.71(2)

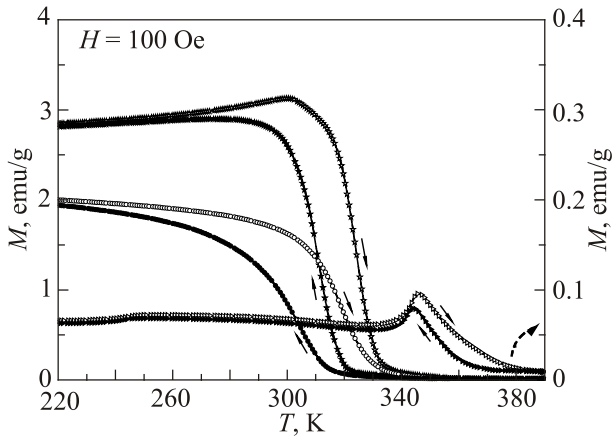


Fig. 2. The $M(T)$ curves for the hardened $\text{NiMn}_{1-x}\text{Cr}_x\text{Ge}$ samples: for $x = 0.04$ (\blacktriangleright , \triangleright , right y axis); $x = 0.18$ (\star , \star); $x = 0.25$ (\circ , \bullet , left y axis). Arrows indicate the direction of temperature changes (FC — solid symbols and FH — open symbols).

It can be assumed by analogy to the $\text{CoMn}_{1-x}\text{Cr}_x\text{Ge}$ and $\text{NiMn}_{1-x}\text{Cr}_x\text{Ge}_{1.05}$ alloys [4,5] that the changes of magnetic properties in the compounds studied as a function of temperature and Cr content are connected with changes of the lattice constants and Mn–Mn interatomic distance.

To determine the temperatures and the nature of crystallographic and magnetic phase transitions in the $\text{NiMn}_{1-x}\text{Cr}_x\text{Ge}$ alloys, the differential scanning calorimetry (DSC) measurements were performed (Fig. 3). The exothermic and endothermic peaks are observed during heating and cooling cycles for all the systems.

The DSC curves for the $\text{Mn}_{0.96}\text{Cr}_{0.04}\text{NiGe}$ alloy show anomalies at 344 K (heating) and 342 K (cooling) corresponding to the magnetic phase transition. The transition from the hexagonal to orthorhombic structure is observed in DSC curves at 380 K while heating and 360 K while cooling. The thermal hysteresis of 20 K confirms the first-order nature of the crystallographic transformation.

For the $\text{Mn}_{0.82}\text{Cr}_{0.18}\text{NiGe}$ alloy, small intensity maxima corresponding to the structural transition at $T_{\text{str}} = 380/360$ K (heating/cooling) and the magnetic transition at $T_N = 345/343$ K (heating/cooling) is probably derive from impurity of compound with small concentration Cr (see above). The strong intensity maxima at $T_C = 330/315$ K

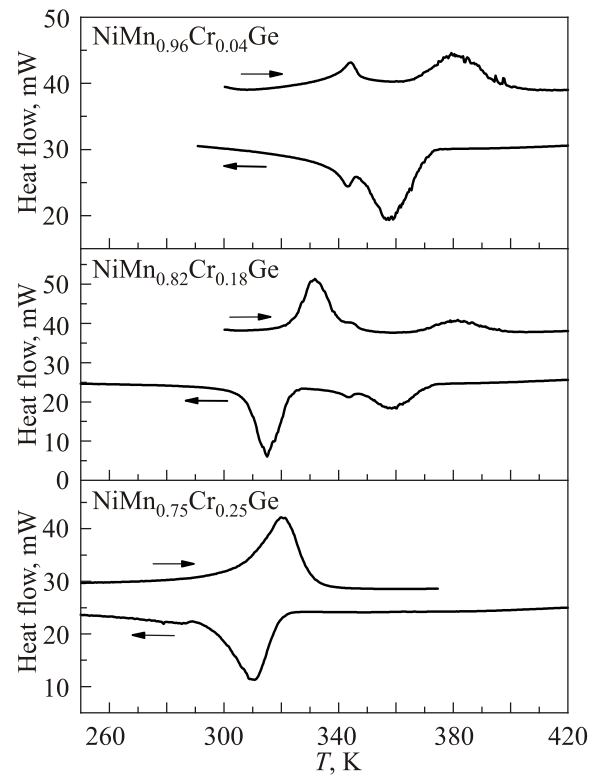


Fig. 3. The DSC heat flow curves as a function of temperature for $(\text{Mn}_{1-x}\text{Cr}_x)\text{NiGe}$ obtained for cooling and heating cycles as indicated by the arrows.

(heating/cooling) is a first-order magnetostructural transition from the combined two-phase FM–PM and the hexagonal and orthorhombic structures.

For the $\text{Mn}_{0.75}\text{Cr}_{0.25}\text{NiGe}$ alloy a first-order magnetostructural transition is observed at 320/310 K. The thermal hysteresis of $T_{\text{hys}} = 10$ K clearly evidences the first-order nature of this transition, which is attributed to the intimate coupling between the paramagnetic and ferromagnetic states and the hexagonal-orthorhombic structural transition.

In the investigated alloys the temperature of martensite transition, T_m , decreases as a result of the joint action of doping by chromium and solid phase hardening. Therefore in these alloys a stability region of high-temperature hexagonal Ni_2In -type phase expands toward the low temperatures and is partially retained below the temperature of the martensitic structural transition (similar situation is observed in $\text{Mn}_{1-x}\text{Cr}_x\text{CoGe}$ [4]).

Table 2. Magnetic data for the quenched $\text{NiMn}_{1-x}\text{Cr}_x\text{Ge}$ system. $T_{N,C}$ is the magnetic ordering temperature (Néel or Curie), Θ is the paramagnetic Curie temperature, ΔT_{hys} is the thermal hysteresis at $T_{N,C}$, $-\Delta S_M^{\text{max}}$ is the magnetic entropy change at the phase transition for $\Delta H = 0\text{--}60$ kOe, μ_{amm} is the average magnetic moment in magnetic field $H = 60$ kOe at $T = 300$ K and μ_{eff} is the effective magnetic moment

Content, x	$T_{N,C}$, K	Θ , K	ΔT_{hys} , K	$-\Delta S_M^{\text{max}}$, J/(kg·K)	μ_{amm} , μ_B	μ_{eff} , μ_B
0.04	344	345	4	5.0	1.11	2.6
0.18	310	318	13	13	1.45	3.9
0.25	305	316	17	23	1.88	3.4

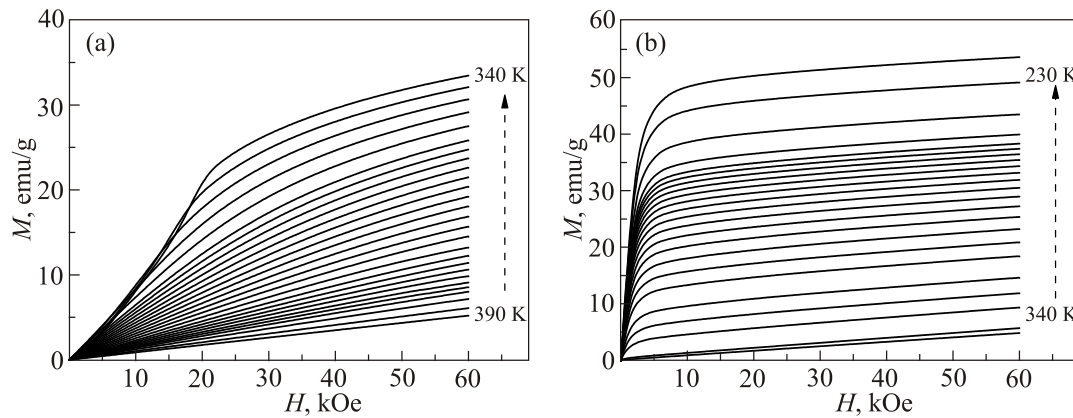


Fig. 4. Field dependences of magnetization at selected temperatures near the phase transition for the samples with $x = 0.04$ (a) and 0.25 (b).

The changes of both temperature of magnetic transition with the increasing Cr concentration and temperature hysteresis of heat flow between heating and cooling cycles are consistent with the magnetization study results.

5. Magnetocaloric effect

For all the samples the field dependences of magnetization have been measured at applied magnetic fields up to 60 kOe in the temperature range of 230–390 K. As an illustration, in Fig. 4(a),(b) the isothermal magnetization curves versus magnetic field at selected temperatures near

the magnetic phase transition are presented for the alloys with small ($x = 0.04$) and large ($x = 0.25$) Cr content, respectively. The magnetization curves for the samples with $x = 0.18$ have similar character to those for $x = 0.25$ (they are not shown).

Figure 4(a) presents the magnetization curves for the samples with $x = 0.04$. It is clearly seen that a behavior of the $M(H,T)$ curves is typical for antiferromagnetic ordering.

Two step-like magnetic transitions can be clearly seen for the sample with $x = 0.04$. The magnetization curves vs. external magnetic field are characterized by a linear in-

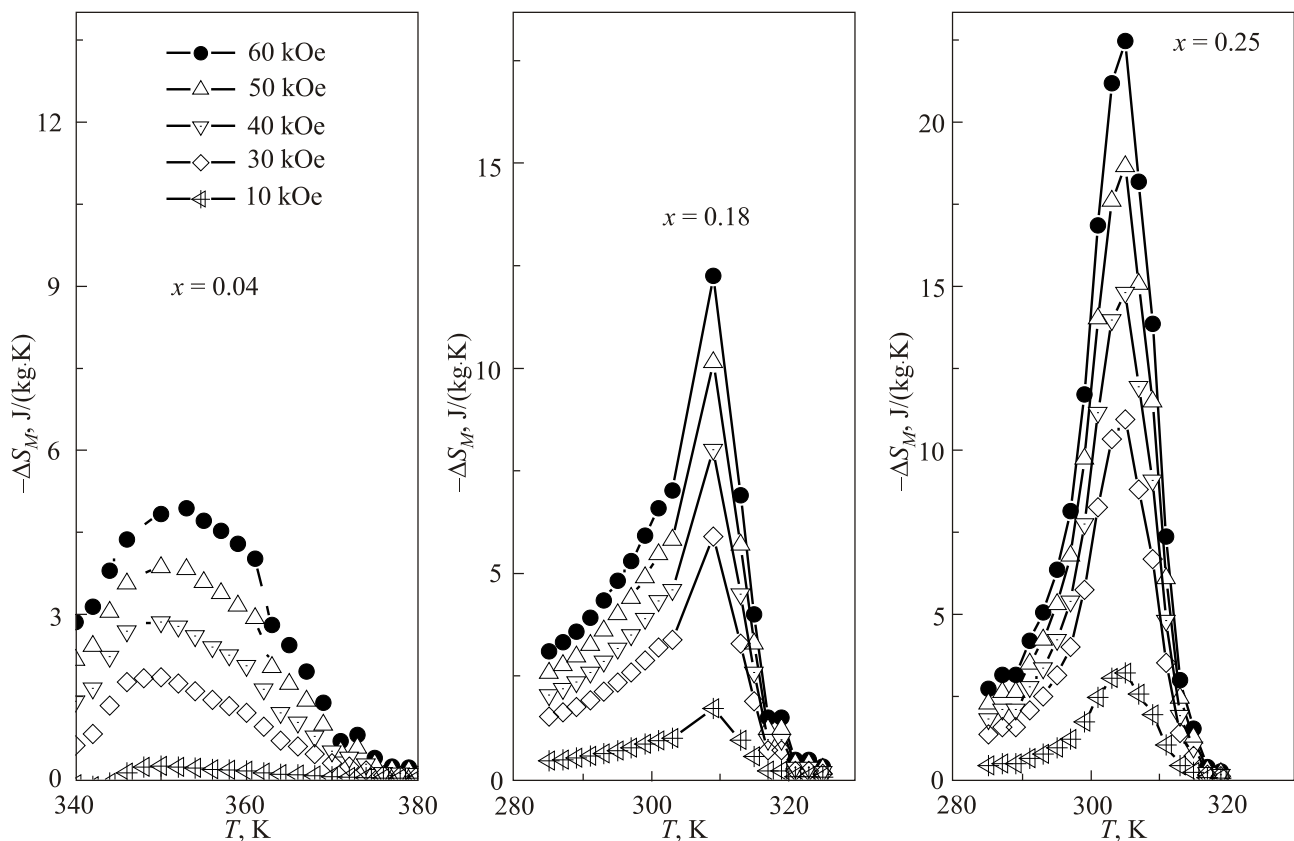


Fig. 5. Temperature dependences of ΔS_M near the magnetic phase transition for the hardened samples with $x = 0.04$, 0.18 , 0.25 for a field change of $\Delta H = 0\text{--}60$ kOe.

crease up to critical field, H_{cr} , and then by another linear growth up to saturation. The critical field values are equal to 5 kOe at $T = 340$ K.

Figure 4(b) clearly shows that the magnetization curves for the sample with $x = 0.25$ demonstrate a behavior typical for ferromagnetic ordering.

A comparison of the $M(H,T)$ curves for the samples studied shows that the average magnetic moments for the hardened samples determined from the magnetization measured in magnetic field $H = 60$ kOe at $T = 300$ K increase with increasing Cr content (Table 2).

The magnetic entropy changes (ΔS_M) near the magnetic phase transition as a function of magnetic field and temperature, characterizing the magnetocaloric effect (MCE), were calculated using the thermodynamic Maxwell relation (MR) [16]. According to MR, the total magnetic entropy change, $\Delta S_M(T,H)$, of the magnetic system during the magnetization processes in magnetic field, H , is given by relation

$$\Delta S_M(T, H) = S_M(T, H) - S_M(T, 0) = \int_0^{H_{\max}} \left(\frac{\partial M}{\partial T} \right)_H dH, \quad (1)$$

where T , H_{\max} and M are the temperature, maximum external field and magnetization, respectively. Knowing the $M(H,T)$ dependence, we have found the derivative $\partial M(T, H)/\partial T$, and substituting it in (1) $-\Delta S_M(T, H)$ was calculated. The $-\Delta S_M(T, H)$ dependences around the phase transition at various external magnetic fields are presented in Fig. 5.

The calculated magnetic entropy changes for the samples with $x = 0.04$, 0.18 and 0.25 for a field change of $\Delta H = 0-60$ kOe are presented in Table 2. The maximum magnetic entropy change induced by magnetic field of 60 kOe is largest for the sample with $x = 0.25$ ($-\Delta S_M = 23$ J/(kg·K)).

6. Conclusions

The results of measurements of structural, magnetic and magnetocaloric properties in the $\text{NiMn}_{1-x}\text{Cr}_x\text{Ge}$ half-Heusler compounds with a variation of chromium concentration ($x = 0.04$, 0.18 and 0.25) are presented. An influence of partial substitution of Cr for Mn on the character of structural and magnetic phase transitions in the quenched alloys has been studied.

The values of temperature of the structural and magnetic phase transitions in the quenched samples are lower than in slowly cooled ones (see Fig. 1 in Ref. 14). Similar effect was observed in $\text{Mn}_{1-x}\text{Cr}_x\text{CoGe}$ [4] and probably is a result of the different homogeneity and chemical order.

A quenching of the $\text{NiMn}_{1-x}\text{Cr}_x\text{Ge}$ alloys results in the transformation of the phase composition of these samples from practically single phase state with an orthorhombic crystal structure for $x = 0.04$ to two-phase (orthorhombic

and hexagonal) state for $x = 0.18$ and 0.25. The studies have shown that the replacement of Mn atoms by Cr ones leads to occurrence and stabilization of the ferromagnetic state. In the quenched samples the magnetostructural phase transition realizes. In contrary to the slowly cooled samples the hardened compounds exhibit a thermal hysteresis in the vicinity of the magnetic and structural phase transitions, which is characteristic for a first-order transitions. The magnetic phase transition temperatures decrease strongly in the hardened alloys at substitution of Mn ions for Cr ones. The magnetic entropy changes, $|\Delta S_M^{\max}|$, obtained for the hardened alloys have the maximum value equal to 23 J/(kg·K) near the magnetic phase transition for a field change of $\Delta H = 0-60$ kOe.

The large magnetocaloric effect makes these materials one of the most promising candidates as working material in magnetic refrigerators.

Acknowledgments

We gratefully acknowledge Dr. T. Jaworska-Gołąb for kind perform XRD measurements and discussion. Financial support of the European Fund for Regional Development (Contract No. UDA-POIG.01.03.01-00-058/08/00) and by the National Centre for Research and Development Research Project no. PBS2/A5/36/2013 is gratefully acknowledged. This work was partially performed in the laboratories equipped by the European Union within the Innovative Economy Operational Program POIG.02.02.00-00-025/09, the European Regional Development Fund in the framework of the Polish Innovation Economy Operational Program contract no. POIG.02.01.00-12-023/08 and the European Regional Development Fund Operational Program Infrastructure and Environment contract no. POIS 13.01.00-00-062/08.

1. V. Markovich, A. Wiśniewski, and H. Szymczak, *Magnetic Properties of Perovskite Manganites and their Modifications*, Handbook of Magnetic Materials, Vol. 22, 1 (2014).
2. O. Tegus, E. Brück, K.H.J. Buschow, and F.R. de Boer, *Nature (London)* **415**, 150 (2002).
3. C.L. Zhang, J. Chen, T.Z. Wang, G.X. Xie, C. Zhu, and D.H. Wang, *Solid State Commun.* **151**, 1359 (2011).
4. N.T. Trung, V. Biharie, L. Zhang, L. Caron, K.H.J. Buschow, and E. Brück, *Appl. Phys. Lett.* **96**, 162507 (2010).
5. C. Zhang, D. Wang, Q. Cao, S. Ma, H. Xuan, and Y. Du, *J. Phys. D: Appl. Phys.* **43**, 205003 (2010).
6. A. Quetz, B. Muchharla, T. Samanta, I. Dubenko, S. Talapatra, S. Stadler, and N. Ali, *J. Appl. Phys.* **115**, 17A922 (2014).
7. A.P. Sivachenko, V.I. Mityuk, V.I. Kamenev, A.V. Golovchan, V.I. Val'kov, I.F. Gribanov, *Fiz. Nizk. Temp.* **39**, 1350 (2013) [*Low Temp. Phys.* **39**, 1051 (2013)].
8. T. Jaworska-Gołąb, S. Baran, R. Duraj, M. Marzec, V. Dyakonov, A. Sivachenko, Yu. Tyvanchuk, H. Szymczak, and A. Szytuła, *J. Magn. Magn. Mater.* **385**, 1 (2015).
9. V. Johnson, *Inorg. Chem.* **14**, 1117 (1975).
10. S. Anzai and K. Ozawa, *Phys. Rev. B* **18**, 2173 (1978).

11. A. Szytuła, Z. Tomkowicz, W. Bażela, J. Todorović, and A. Zięba, *Physica B* **86–88**, 393 (1977).
12. W. Bażela, A. Szytuła, J. Todorović, Z. Tomkowicz, and A. Zięba, *Phys. Status Solidi (a)* **38**, 721 (1976).
13. W. Bażela, and A. Szytuła, *Phys. Status Solidi (a)* **66**, 45 (1981).
14. A. Szytuła, S. Baran, T. Jaworska-Gołąb, M. Marzec, A. Deptuch, Yu. Tyvanchuk, B. Penc, A. Hoser, A. Sivachenko, V. Val'kov, V. Dyakonov, and H. Szymczak, *J. Alloys Compd.* **726**, 978 (2017).
15. K. Pecharsky and K.A. Gschneidner, Jr., *Phys. Rev. Lett.* **78**, 4494 (1997).
16. V.K. Pecharsky and K.A. Gschneidner, Jr., *J. Magn. Magn. Mater.* **200**, 44 (1999).

Вплив заміщення Mn на Cr на магнітокалоричні властивості загартованих сплавів $\text{NiMn}_{1-x}\text{Cr}_x\text{Ge}$

Е. Зубов, М. Неділько, О. Сіваченко, К. Д'яконов, Ю. Тиванчук, М. Marzec, В. Вальков, W. Bażela, A. Ślawska-Waniewska, В. Д'яконов, А. Szytuła, Н. Szymczak

Досліджено кристалографічні, магнітні, термомагнітні та магнітокалоричні властивості загартованих half-Heusler сплавів $\text{NiMn}_{1-x}\text{Cr}_x\text{Ge}$ ($x = 0,04, 0,18$ та $0,25$) за допомогою рентгенівської дифракції, диференціальної скануючої калориметрії та

вимірювань намагніченості. Вивчено вплив часткової заміни Cr на Mn та гартування зразків на характер структурних та магнітних фазових переходів. Гартування сплавів призводить до утворення двофазної (ромбічної й гексагональної) кристалічної структури. Магнітні властивості досліджувалися за допомогою вимірювань намагніченості в широкому діапазоні температур (5–400 K) і магнітного поля (до 60 кЕ). Експериментальні дані показують, що при гартуванні та збільшенні вмісту Cr магнітне впорядкування змінюється від антиферомагнітного до феромагнітного. Загартовані сполуки виявляють тепловий гістерезис поблизу магнітного фазового переходу, що характерно для магнітного фазового переходу першого роду. Температури магнітного фазового переходу зменшуються в результаті загартування зразків. Зміни магнітної ентропії розраховано з використанням польових залежностей ізотермічної намагніченості в термінах термодинамічного співвідношення Максвелла. Зміна магнітної ентропії, $|\Delta S_M^{\max}|$, отримана для зміцнених сплавів з $x = 0,25$, має максимальне значення 23 Дж/(кг·К) поблизу магнітного фазового переходу при зміні поля $\Delta H = 0\text{--}60$ кЕ.

Ключові слова: інтерметалеві сплави $\text{NiMn}_{1-x}\text{Cr}_x\text{Ge}$, намагніченість, магнітний фазовий перехід, магнітна ентропія, магнітокалоричний ефект.